

MATERIALS RESEARCH FOR THE CLEAN UTILIZATION OF COAL

QUARTERLY PROGRESS REPORT

April - June 1980

Samuel J. Schneider  
Project Manager

Center for Materials Science  
National Bureau of Standards  
U. S. Department of Commerce  
Washington, D. C. 20234

PREPARED FOR THE UNITED STATES  
DEPARTMENT OF ENERGY

Office of Advanced Research and Technology

Under Contract No. EA-77-A-01-6010

"This report was prepared as an account of work sponsored by the United States Government. Neither the United States nor the United States Department of Energy, nor any of their employees, nor any of their contractors, subcontractors, or their employees, makes any warranty, expressed or implied, or assumes any legal liability or responsibility for the accuracy, completeness, or usefulness of any information, apparatus, product or process disclosed, or represents that its use would not infringe privately owned rights."



## TABLE OF CONTENTS

	PAGE
I. SUMMARY OF PROGRESS TO DATE . . . . .	1
II. DETAILED DESCRIPTION OF TECHNICAL PROGRESS. . . . .	2
1. Materials Performance and Properties . . . . .	2
2. Creep of MHD Refractories. . . . .	2
3. Electrical Transport Mechanisms in Slag. . . . .	3
4. Corrosion of Downstream MHD Components . . . . .	14



## I. SUMMARY OF PROGRESS TO DATE

### Brief Summary

#### 1. Materials Performance and Properties

A large portion of the data for the book on construction materials for coal gasification was assembled; final cost information was received from computer vendors for services required for the data base computer management; the Failure Information Center transmitted 791 abstracts, 27 tables, and one hard copy report to industry; a report on erosive failures in coal conversion pilot plants will be published as an NBS Internal Report.

#### 2. Creep and Related Properties of MHD Refractories

Work during the quarter was concentrated on assembling the 12 station creep assembly. Compressive yield results were obtained on two materials, magnesia excess spinel and a sodium doped alumina at 1400 °C, and 1500 °C. Both materials were relatively creep resistant.

#### 3. Electrical Transport Mechanisms in Slag

The electrical conductivity of a slag containing 20 percent by weight of  $\text{Fe}_3\text{O}_4$  has been completed. The data reinforces the suggestion that the primary conducting mechanism in iron-containing slags at high temperature is iron ion conductivity. A paper detailing the information leading to this conclusion was given at the 7th International Conference on MHD Electrical Power Generation, held at MIT, Cambridge, Mass., June 16-20, 1980.

#### 4. Corrosion of Downstream MHD Components

Type 316 and Type 304 stainless steel tubes were exposed for 4 hours to various oxygen/fuel ratios and  $\text{K}_2\text{SO}_4/\text{K}_2\text{CO}_3$  seed combinations. These data indicate that seed could cause tube fouling; fouling extent differs under the various test conditions. Wastage evaluations, started last quarter, indicate that Type 304 stainless steel corrodes (weight loss) at the rate of about 4 mm per year.

## II. DETAILED DESCRIPTION OF TECHNICAL PROGRESS

### 1. Materials Performance and Properties (H. M. Ondik, R. C. Dobbyn, A. Perloff, W. S. Brower, and W. A. Willard)

Progress: The normal collection and evaluation of materials performance and properties data has continued along with preparation of data tables for the book on construction materials for gasification use. At two separate times during the quarter, the beginning, and two-thirds through, the completed tables for the book were assembled. Currently, all of the data available from the Failure Information Data Base has been tabulated and arranged, and entered into the Plant Experiences subsections of Section A of the book. Tables for Section B, containing data for DOE research contractors' reports are not quite complete, but work is continuing. The "Operating Requirements" portions of Section A are being assembled.

The Failure Information Center received twelve requests for information during the quarter. In response to these requests a total of 791 abstracts, 27 tables and one hard copy report were transmitted. Also during this quarter the final draft of a report addressing erosive wear failures was delivered to DOE; this report will also be published as a NBS Internal Report, NBSIR 80-2045.

Main Commerce is currently evaluating the final cost figures provided by computer vendors who have submitted bids for the services we wish to obtain. There have been a variety of delays during the quarter, most of them due to vendors asking for time extensions. It should be a matter of days only and the winner of the award will be known. Perhaps two months after that date the contract will be signed and in effect. Training for Data Center personnel in the use of the Data Base Management System will then begin.

Plans: The book on construction materials for gasification is to be completed; normal acquisition and dissemination of data will continue. The computer services contract should be awarded and training in the use of the system will begin.

### 2. Creep and Related Properties of MHD Refractories (N. J. Tighe and C. L. McDaniel)

Progress: Work during the quarter concentrated on assembling the 12 station creep assembly while continuing the creep yield experiments on the excess magnesia-spinel and the sodium doped alumina refractory.

The 4 creep furnaces are being fitted with a water-cooled drive rod assemblies for the attachment to the load cells and to the pneumatic cylinders. Preliminary tests with the one inch rods in place indicate that the excessive heat loss through these rods reduced the maximum temperature to  $< 1600^{\circ}\text{C}$ . With the  $3/4$  inch rods the desired furnace temperature could be reached. Since both sizes of rods are in hand the  $3/4$  rods will be used for the highest temperature. Modification of the furnaces is being discussed with the manufacturer. The fixtures should be in place in all the furnaces when the power supply console is delivered in July.



Creep tests on selected refractories included:

Chrome-spinel - Results obtained on this material were presented in the Refractories Division at the American Ceramic Society Meeting in April. An NBSIR Report will be issued on this material.

Magnesia Excess Spinel - Creep yield tests on this material were carried out at a constant loading rate of  $2 \times 10^{-4}$  in/min at 1400 °C, 1500 °C and 1600 °C. The results indicate a moderate yield drop.

Sodium Doped Alumina: This material was received from K Keto of Montana Tech in the form of cores taken from bricks installed in the test reactor at Montana State U. Creep yield tests were carried out at 1400 °C and 1500 °C at the constant load rate of .002"/min. At 1400 °C the material is very creep resistant but there is a 3-fold drop in yield stress at 1500 °C compared with the results at 1400 °C. The X-Ray analysis of the material showed it to be composed of  $\alpha$  and  $\beta$  alumina. There is a gradual loss of  $\beta$  during the high temperature exposure.

Plans: During the next quarter the power supply should be delivered and put in service with the 12 station creep assembly. A differential displacement device will be evaluated for measuring the creep rate in the new creep assembly.

The reaction of the sodium-doped material with slag in the Montana State test rig will be evaluated and compared with the results obtained from the creep tests.

The inclusion of an NBS representative on the air-preheater materials selection committee will be explored. Although this committee was only informally established in FY 79, its usefulness to the selection and evaluation of air-preheater materials has been demonstrated by the progress obtained to date.

### 3. Electrical Transport Mechanisms in Slag (W. R. Hosler)

#### Progress:

##### Slag Electrical Conductivity

In order to further investigate the effect of iron on the electrical conductivity of coal slag in relationship to other slag components, and in relationship to the redox conditions surrounding the material, an additional batch of slag from the Bow, NH steam generating plant (but containing extra iron) has been prepared. Iron was added in the form of  $\text{Fe}_3\text{O}_4$  to bring the total iron content to 20 mass percent. This material is difficult to form in the measuring crucible and must be formed in a reducing atmosphere before contacts are attached. (See below for an explanation of contacting procedure and four probe DC measurements.) The conductivity measurements on this material have been completed and the data is given in Figures 1 and 2. As in all previous measurements on this slag, there is a break point in the curve above

1385 °C ( $1/T(K) \approx 6 \times 10^{-4}$ ) and all samples show nearly the same slope of conductivity vs. reciprocal temperature regardless of the iron or potassium content and regardless of the ambient oxygen pressure. It is evident, however, that the magnitude of the conductivity in this temperature range is larger than for the data on Bow, NH slag reported in previous quarterly reports beginning April - June 1979 except for that slag sample containing an even larger amount of iron (23.4%) reported in the last quarterly report for Jan. - March 1980. Table 1 gives the conductivity at 1450 °C of all the samples measured to date. The analyses shown are based on the original analysis of this slag as received from the Bow, NH steam plant. This original analysis is given in Table 1, page 33 of QR April - June 1979.

Table 1

Based on Initial Analysis		Conductivity At 1450 °C (ohm-cm) <sup>-1</sup>	
Mass % Fe	Mass % K	Air	5 ppm O <sub>2</sub>
14.7	0.43	0.066	0.062
12.8	8.4	0.058	0.066
23.4	7.5	0.31	
20.0	0.40	0.16	0.16

The data shown in Figures 1 and 2 show the same general characteristics below 1385 °C as the previous data on this slag shown in QR April - June 1979 when the data is taken according to a prescribed routine which was designed to freeze in a specific ratio of iron ions ( $Fe^{+2}/Fe^{+3}$ ) below 1000 °C. The previous sample contained only 14.7% iron and the conductivity on the lower branch of the conductivity curves (below 1000 °C) is about an order of magnitude lower than for the data shown in Figure 1. The high conductivity branch of the curves, however, are similar in magnitude as well as shape. A preliminary investigation using SEM analyses of material providing the data for these low temperature branches of the curves (below 1000 °C) indicates that the conductivity is not primarily a function of the  $Fe^{+2}/Fe^{+3}$  ratio frozen in by the quench to 900 °C (see QR April - June 1979) but is due mostly to the crystalline component of the solidified slag. Scanning electron microscope micrographs show crystallite bridging in various degrees depending on the history of the sample. It is possible that this bridging accounts for the somewhat unpredictable conductivity below 1000 °C particularly since there does not seem to be a primary dependence of the conductivity on the oxygen pressure (vis. Fig. 1 and



2). This concept is being investigated and will be reported on at a later time. A paper was presented at the 7th International Conference on MHD, held at MIT in Cambridge, June 16 - 20, 1980, Session 5, Paper No. D - 7 which gives a possible explanation for the high temperature behavior (above 1385 °C) of iron-containing slags. It can readily be seen from Table 1 that the conductivity at 1450 °C depends on the iron content and not on the amount of potassium (for the several amounts shown in the table) and not on the oxygen partial pressure in the range from 0.2 to  $10^{-6}$  atmospheres. The conclusion drawn then is that for this slag composition, the conductivity above 1385 °C is due primarily to the iron ions.

### Measurement Technique and Sample Preparation

Measurements of the physical properties of materials at high temperatures are becoming increasingly important particularly with respect to emerging energy technologies. A few examples include materials used in magneto-hydrodynamics, fuel cells, and batteries for energy storage and conversion of chemical to electrical energy. The electrical conductivity of some materials for these technologies is important as all require the passage of current (ionic and/or electronic). For those materials that remain solid with relatively simple chemistry in a device, the conductivity measurement over the useful temperature range is not difficult. However, for those materials that may be in a solid and/or liquid state, depending on temperature, the measurement becomes more difficult. Measurements are complicated further by chemical interaction of a material with the containing crucible, by chemical/phase changes with temperature and oxygen pressure, by thermal expansion or contraction problems upon solidification or cooling, and by the requirement of electrical contacts that will give reliable results without disintegration. A measurement technique has been developed over the last year which can alleviate these problems. A brief description of the sample preparation and measurement technique both of which are extremely important for obtaining valid results on high temperature materials such as coal slag follows. Generally, only four probe DC conductivity measurements will be discussed. Two probe DC measurements give erroneous results when ionic conductivity is involved, especially when ion exchanging electrodes are not used. AC measurements are useful for samples having relatively high resistances where capacitive reactance components can be determined at reasonable frequencies (< several megahertz). For most high temperature materials, however, the electrical conductivities are high enough ( $\sim 0.01$  to  $10 \text{ ohm}^{-1}\text{cm}^{-1}$ ) so that the required frequencies are too high to resolve the capacitive-reactive components of the total impedance which are due to contact barrier layers or grain boundary effects. Four probe AC measurements, however, are a viable option but usually require more instrumentation than DC measurements.

For materials which can be cut to a suitable sample size and will not flow over the temperature range of the measurement, contacts can be applied directly to the material by drilling small holes (diamond dental drill) in the sample to attach the contact lead wires. This is done by

peening spongy platinum around the leadout wires, which are usually platinum to withstand the high temperature oxidizing atmospheres. A schematic diagram of a typical contact is shown in Figure 3. Generally the portion of the wire in the hole should have a non-symmetrical configuration on the end to prevent the wire from turning in the hole and to prevent pull-out from the adjacent peened platinum. In the schematic, an oval disk is shown. This was made by inserting the leadout wire with a small ball on the end through a hole in a piece of metal and simply hammering the ball flat. Any non-symmetrical shape formed in any way will suffice. Measurements using this contacting method have been made on many ceramic materials up to 1700 °C. No contact resistances were apparent. For best results, the materials should be fully sintered up to the highest measuring temperature to prevent further densification during measurement. Figure 4 shows a radiograph of a sample of  $Y_{0.95}Ca_{0.05}CrO_3$  with contacts applied as described above.

For a material such as slag that becomes molten within the range of temperatures involved in the measurement, a different procedure was used. Alumina crucibles which are readily available and which show minimal reaction with the slag were chosen for the experiments. A crucible is carefully filled to just under one-half full by repeated melting of additions of slag powder. This is necessary to prevent the material with absorbed gases from bubbling over the top during the initial filling process. Holes are then drilled through the crucible sides and into the slag for the four probes. Leads are attached using the same procedure as described above. Figure 5 shows a radiograph of a typical crucible with leads attached and numbered for the discussion to follow.

Spongy platinum is commercially available from several companies specializing in platinum products. It can readily be made, however, from powdered platinum which is sintered lightly at 1200 °C for 1/2 hour. The resulting spongy solid mass can be cut into pieces and can be pressed into the holes surrounding the leadout wires. For small samples such as described above, the contacting must be done under a binocular microscope. The peening tools can be made from any hardened metal material formed into a suitable tip for compaction of the spongy platinum. This method yields a leak tight seal.

It can be seen (Fig. 5) that the size and shape of the molten sample remains fixed during the course of the measurement. This is essential for accurate determination of a conductivity. Furthermore, the electrodes do not penetrate a surface exposed to the ambient atmosphere so that oxidation-reduction conditions at the surface do not affect the conductivity value.

The measurements are made using a constant current power supply. In certain temperature ranges and under certain conditions the material is an ionic conductor. Under these circumstances, care must be taken during data acquisition to avoid polarization on the conductivity probes (two center probes). Since the current is maintained constant, the voltage measured between the conductivity probes is a true measure of the bulk conductivity of the material, i.e.,  $\sigma = 1/\rho = \ell I/AV_{23}$  where A is



the cross sectional area of the sample,  $\ell$  is the distance between the conductivity probes 2 and 3, and  $V_{23}$  is the potential developed between the conductivity probes 2 and 3 at a constant current  $I$ . This conductivity may be electronic and/or ionic depending on the chemical (bulk and phase) and physical state of the material, but  $V_{23}$  will remain constant with time. If there is no potential drop at the current contacts (contacts 1 and 4, Figure 5) due to a contact resistance and the conductivity is entirely electronic, no polarization with time will be observed at a given temperature on all probe sets  $V_{12}$ ,  $V_{23}$ ,  $V_{34}$ , or  $V_{14}$ . If the conductivity is ionic or partially ionic and probe measurements are taken in a reasonably short time at low electric fields ( $< 1\text{V/cm}$ ) such that polarization effects do not extend far beyond the current carrying contacts 1 and 4, probe voltage  $V_{23}$  will remain constant but  $V_{12}$ ,  $V_{34}$  and  $V_{14}$  will change with time during the short interval that current is flowing for the measurement. With the data acquisition system (D.A.S.) used in this experiment, collecting a set of data points (i.e.,  $V_{12}$ ,  $V_{23}$ ,  $V_{34}$ ,  $V_{14}$ , temperature, current, and time) required about 40 seconds for one applied voltage polarity. Since the current is reversed for each data point at a given temperature to eliminate permanent polarization build up at any current carrying electrode and to eliminate any thermoelectric voltage present due to a temperature gradient along the length of the sample, the total time to scan all voltages for both current directions is approximately 80 seconds. The D.A.S. consists of a programmable calculator-based system interfaced with appropriate electrometers and voltmeters to measure the necessary parameters. The data can be stored and calculations are made automatically after the current is off.

All conductivity curves reported during the last year were obtained using this method. These are a reflection of the probe voltage  $V_{23}$  versus the temperature. Each point on the curve is representative of near equilibrium conditions for temperatures above  $1000^\circ\text{C}$ . Since diffusion of oxygen is relatively slow at temperatures below  $1000^\circ\text{C}$ , very long times are required, days or weeks, for complete stabilization and data below this temperature have a quenched-in  $\text{Fe}^{2+}/\text{Fe}^{3+}$  ratio and crystalline content. In addition, for slag samples, precipitation and re-resolution of crystalline phases causes the conductivity to change with time at a given temperature above  $1000^\circ\text{C}$ . These processes generally follow an exponentially decreasing curve. In order to be able to complete the experiment in a reasonable time, a data point was considered close enough to its final equilibrium value when the change in conductivity was less than 1% over a ten minute period. At a given temperature, data was taken at ten minute intervals with applied voltage off between measurements. Above  $1300^\circ\text{C}$  these conditions could be met in less than 1 hour while below  $1300^\circ\text{C}$  durations as long as 20 hours were required. No polarization was observed in this voltage measurement ( $V_{23}$ ) at any time during the run. Since polarization at current carrying contacts can be expected for ionic conductors where the electrodes are not ion exchanging, as is the case here, some information can be obtained by comparing the voltages developed at the probe sets during the course of the data acquisition. A complete description of the information that can be obtained in this manner will be given in a later quarterly report. For best results these scan voltages must be interpreted in conjunction with x-ray diffraction and scanning electron microscope analytical techniques.

## Plans

Electrical conductivity measurements of various slags will continue with particular attention to analysis of the results pointing closely to understanding the conductivity process. The analytical methods described in this report will be extended and hopefully will be applied to four probe AC conductivity data if the equipment on hand will lend itself to this measurement.

In the last quarterly report, an electrochemical study was reported on a slag at 1250 °C. This temperature is below the break point in conductivity (1385 °C) as shown in Figures 1 and 2 of this report on slag containing no added potassium. Voltage breakdown was seen to occur at this temperature (1250 °C) in about 2 minutes in a constant current mode at a current density of 0.2A/cm<sup>2</sup>. This experiment should be repeated at a temperature greater than 1385 °C to determine the effect of decreased viscosity, and hence, increased iron ion conductivity of slag on the time for voltage breakdown.

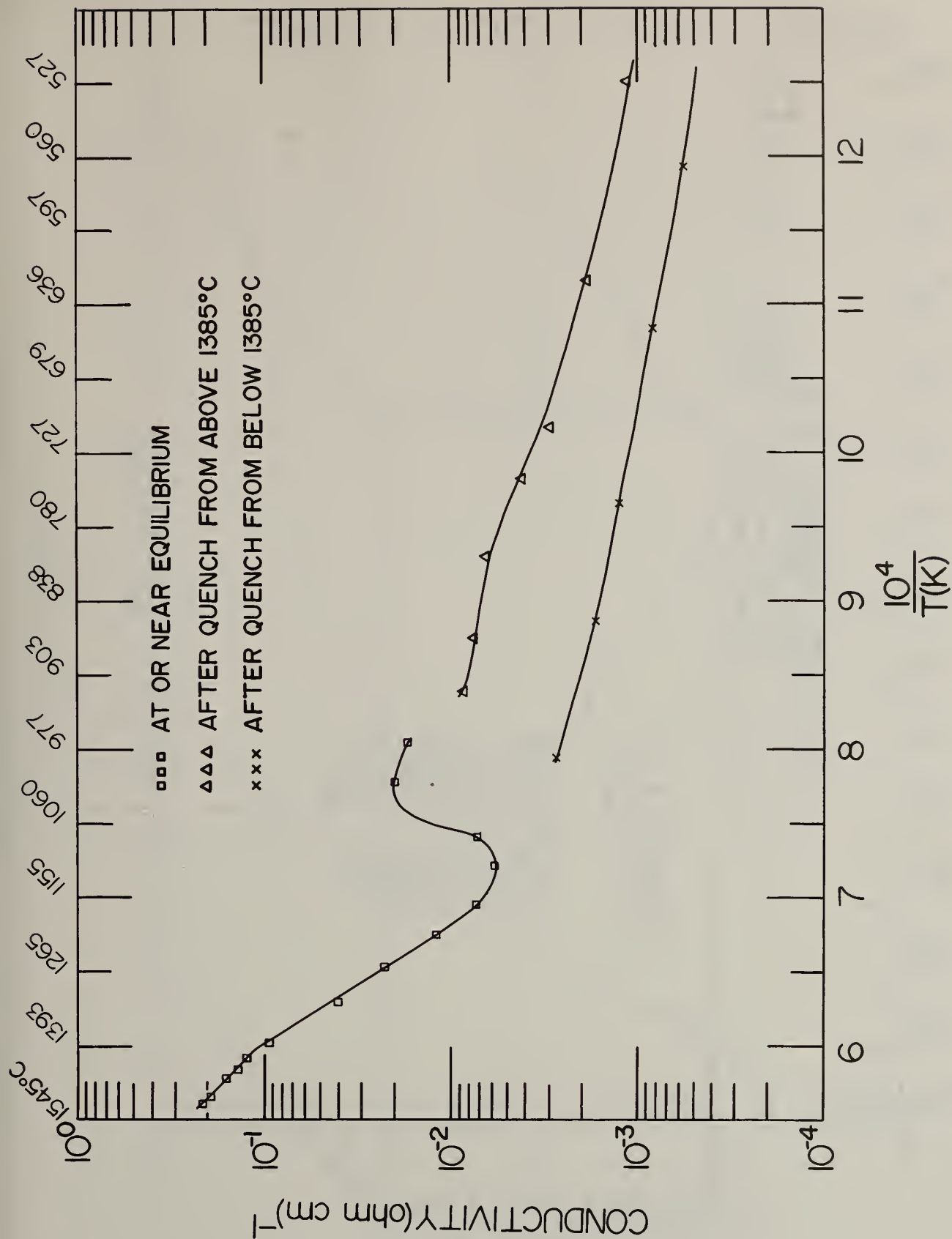


Figure 1. Electrical Conductivity of Bow NH slag containing 20 % Fe as a function of temperature in an air atmosphere.



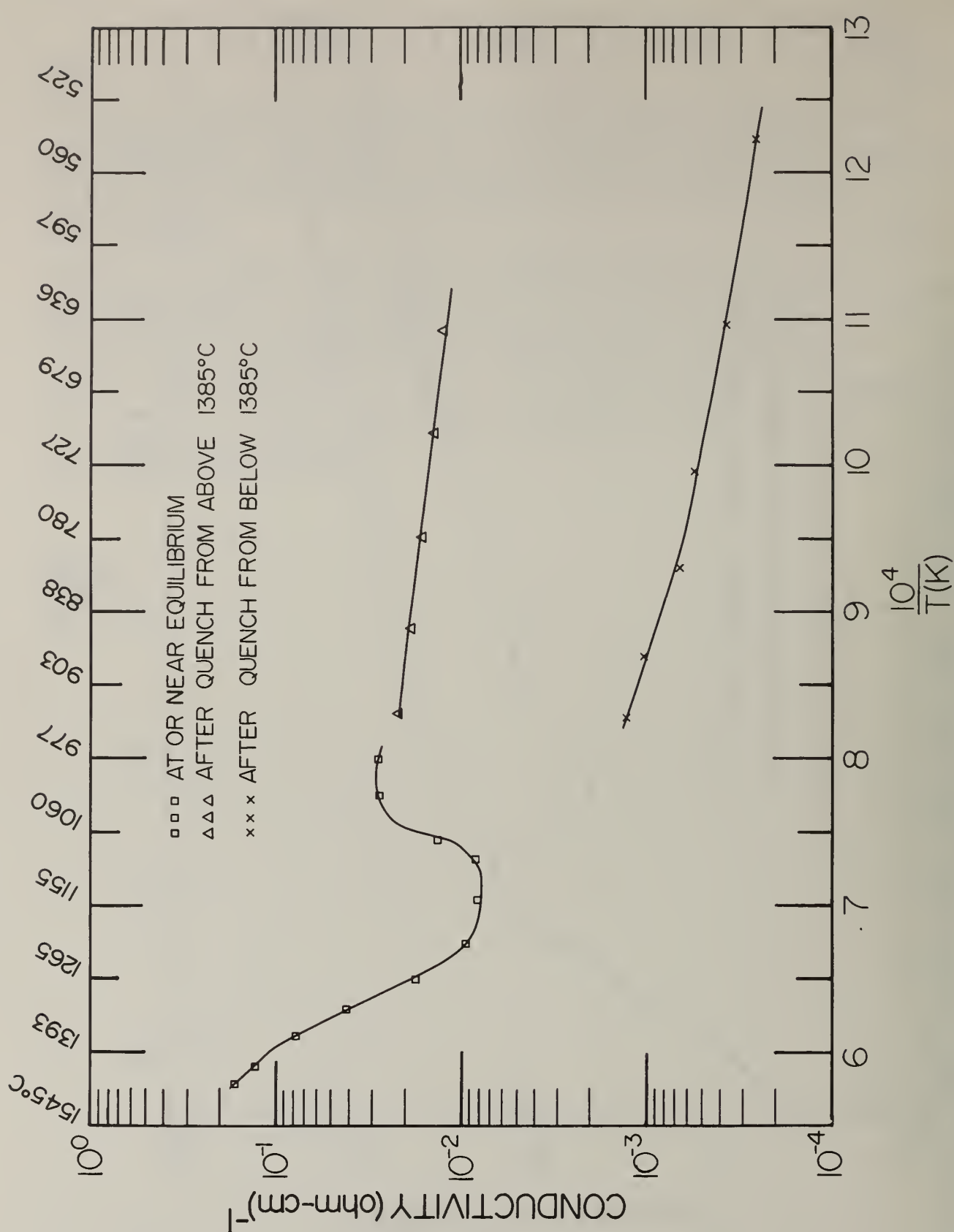


Figure 2. Electrical conductivity of Bow NH slag containing 20 % Fe as a function temperature in an atmosphere of  $5 \times 10^{-6}$  ppm  $\text{O}_2$  in  $\text{N}_2$ .

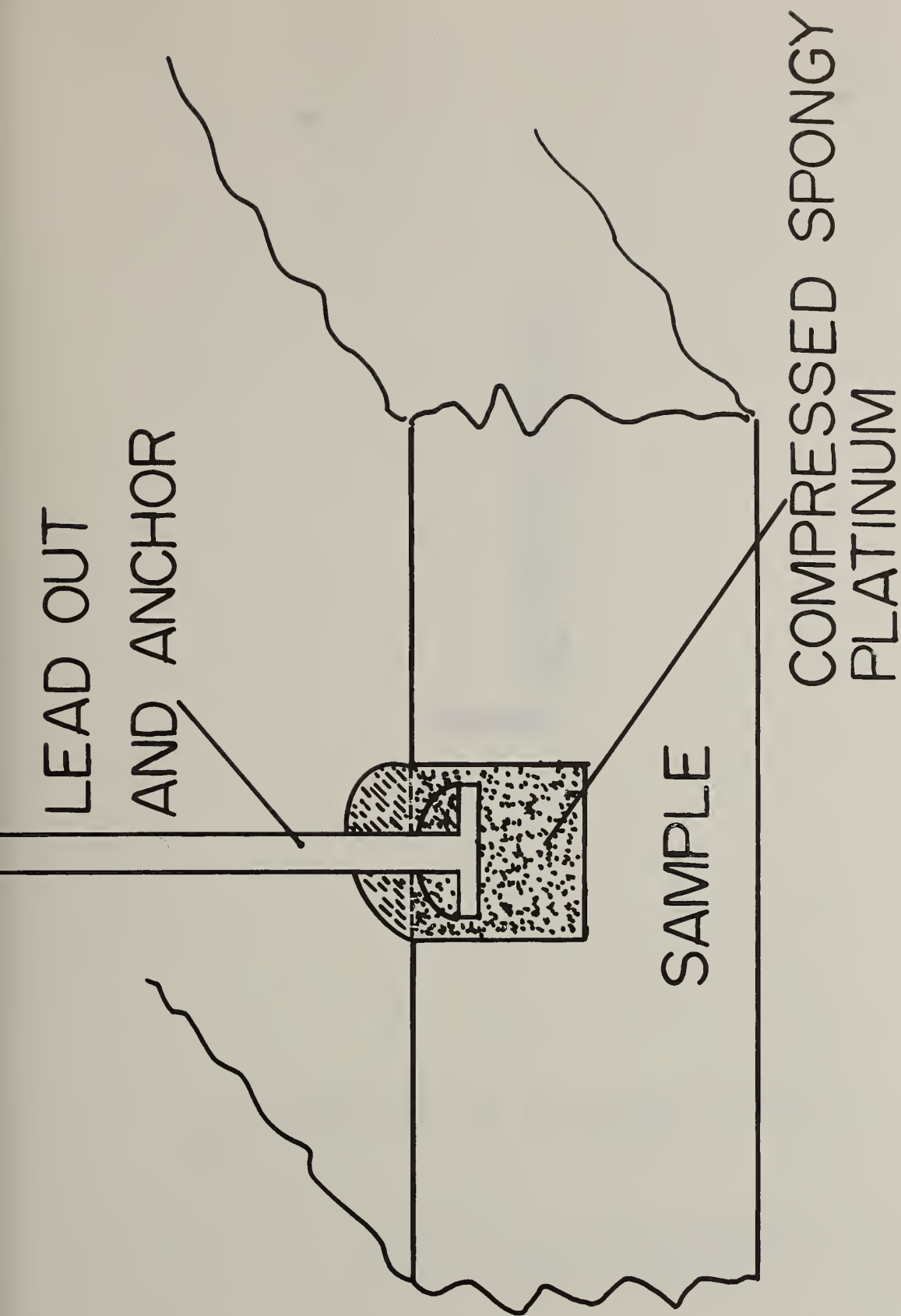


Figure 3. Schematic of typical leadout wire assembly for high temperature electrical conductivity measurements.



Figure 4. Radiograph of sample and leadout wires mounted as illustrated in Figure 3.

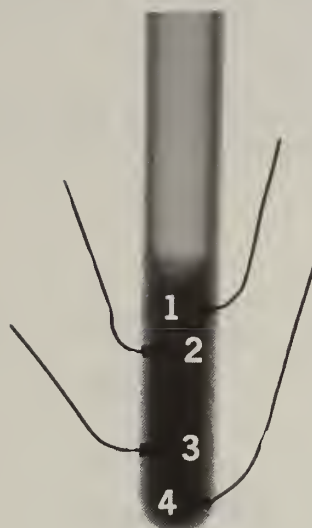


Figure 5. Radiograph of slag sample contained in alumina crucible with leadout wires (numbers) extending through walls.

#### 4. Corrosion of Downstream MHD Components (J. Smit and C. D. Olson)

Progress: Type 316 and Type 304 stainless steel tubular specimens were exposed to seeded oxygen-propane fired hot gas streams at various seed compositions, fuel to oxygen ratios and tube wall temperatures. Exposure time for all specimens, exclusive of apparatus warm-up and cool-down time was four hours. Seeding took place for the first twenty-five minutes of exposure during which approximately 250 grams of seed was added to the hot gas stream. For all specimens the gas stream temperature in the vicinity of the specimen was held at about 1300 °C. Tube wall temperatures, monitored by Pt/Pt10Rh thermocouples welded into the midpoint of the specimens, were maintained at either 500 °C or 590 °C by internal air cooling.

Six specimens of Type 316 stainless steel were exposed in the manner described above and to the specific conditions as indicated in Table 1.

Table 1.

<u>Specimen No.</u>	<u>Wall Temp (°C)</u>	<u>Seed</u>	<u>Gas Stream State</u>
5-6	500	$K_2SO_4$	fuel rich
6-6	590	$K_2SO_4$	fuel rich
7-6	500	$K_2SO_4 + K_2CO_3^*$	$O_2$ rich
8-6	590	$K_2SO_4 + K_2CO_3^*$	$O_2$ rich
9-6	590	$K_2SO_4 + K_2CO_3^*$	fuel rich
10-6	500	$K_2SO_4 + K_2CO_3^*$	fuel rich

\* Ratio of  $K_2SO_4$  to  $K_2CO_3$  is 1:4 by weight.

Following exposure, sections were taken from the specimens for optical, SEM and EDX analysis. The sections, prepared using metallographic techniques, were cut from a location 10 mm away from the midpoint position on the specimen. Because of the sensitivity of the deposited coatings to moisture the tubular specimens were encapsulated immediately upon removal from the test rig. All cutting, grinding, and polishing operations were conducted using non-aqueous media. In addition the sections were stored in vacuum dissicators except during intervals of processing. Figures 1-6 are optical micrographs of specimens 5-6 through 10-6 so handled. The leading tube surface is at the top of each picture. The geometry of the deposited coatings is consistent with that observed on the Type 304 stainless steel tubes at the same conditions and reported on previously.



The nature, size and shape of the deposited coatings is of importance to both the heat and seed recovery aspects of the bottoming steam plant operation. These characteristics will effect not only the heat transfer properties of the system but will also have a major influence on fouling conditions particularly in the main heat exchanger. Further, the removal of this material and its subsequent transport downstream will prove an added burden to the seed recovery system.

Figures 7-18 are micrographs of sections of Type 304 stainless steel reported on earlier showing the deposited coatings. The leading tube surface is at the top of each picture. These specimens were prepared in the same manner as the Type 316 stainless steel tubing described in a succeeding paragraph. The conditions of exposure are given in Table 2 and some conclusions regarding these coatings follow.

Table 2

<u>Figure No.</u>	<u>Wall Temp. (°C)</u>	<u>Seed</u>	<u>Gas Stream Condition</u>
7	400 °C	$K_2SO_4$	$O_2$ rich
8	500 °C	$K_2SO_4$	$O_2$ rich
9	590 °C	$K_2SO_4$	$O_2$ rich
10	400 °C	$K_2SO_4$	fuel rich
11	500 °C	$K_2SO_4$	fuel rich
12	590 °C	$K_2SO_4$	fuel rich
13	400 °C	$K_2SO_4 + K_2CO_3^*$	$O_2$ rich
14	500 °C	$K_2SO_4 + K_2CO_3^*$	$O_2$ rich
15	590 °C	$K_2SO_4 + K_2CO_3^*$	$O_2$ rich
16	400 °C	$K_2SO_4 + K_2CO_3^*$	fuel rich
17	500 °C	$K_2SO_4 + K_2CO_3^*$	fuel rich
18	590 °C	$K_2SO_4 + K_2CO_3^*$	fuel rich

\* Ratio of  $K_2SO_4$  to  $K_2CO_3$  is 1:4 by weight.

Generally a compact seed deposit forms on the leading surface of the tube, being thinnest at the midpoint and broadest at the compact deposit-powdery deposit merge zone. A thinner somewhat powdery deposit forms on the trailing surface. The leading surface deposit is independent of temperature (400 °C - 590 °C) for the case of  $K_2SO_4$  in  $O_2$  rich hot gas streams. For all other cases the deposit thickness decreases with increasing tube wall temperature. Leading surface deposits are generally thicker in  $O_2$  rich hot gas streams while trailing surface deposits are generally thicker in fuel rich hot gas streams. The combination of  $K_2SO_4$  with  $K_2CO_3$  results in a thinner deposit at all temperatures for the  $O_2$  rich hot gas stream case than for the  $K_2SO_4$  alone.

From the preceeding then it may be argued that fouling in the heat exchanger area would probably be least and the heat transfer efficiency greatest at the higher temperature, i.e., above 500 °C, with a  $K_2SO_4 + K_2CO_3$  mixture probably in an oxygen rich hot gas stream.

The gravimetric studies initiated in the last quarter were continued during this reporting period. Three specimens of Type 304 stainless steel tube were exposed at 590 °C to conditions indicated in Table 3. Prior to exposure the specimens were cleaned with ethanol and weighed. Immediately following exposure the specimens were rinsed with warm water and then ethanol to remove the seed deposit. The specimens were then cleaned in a ultrasonic bath with 10%  $HNO_3$  at 50 °C for twenty minutes and reweighed. The weight change is noted in Table 3. Even by the most conservative treatment the weight loss translates to a wastage of 4 mm per year which is not acceptable and would virtually eliminate Type 304 stainless steel as a candidate material.

Plans: Specimens of Type 316 stainless steel previously exposed and prepared will be analyzed by SEM and EDX techniques for signs of both incipient and gross corrosion. In addition deposit samples obtained from specimens exposed for gravimetric analysis will be analyzed using x-ray diffractometer techniques. The purpose of this analysis is to obtain more information on the corrosion process involved and on the possible transformation of the seed compounds during deposition.

Table 3

Specimen No.	Specimen Stainless Type	Seed	Gas Stream State	Specimen Temp. °C	Weight in Grams Before Test	Weight in Grams After Test	Change in Weight in Grams
15-4	304	$K_2SO_4$	fuel rich	590	67.233	67.187	0.046
16-4	304	$K_2SO_4 + K_2CO_3$	fuel rich	590	66.320	66.289	0.031
17-4	304	$K_2SO_4 + K_2CO_3$	$O_2$ rich	590	66.378	66.351	0.027

Fig. 1. Section of Type 316 stainless steel tubing after exposure to  $K_2SO_4$  seeded fuel rich hot gas stream. Note deposit on lower surface. Tube temperature 500 °C. 6 X.

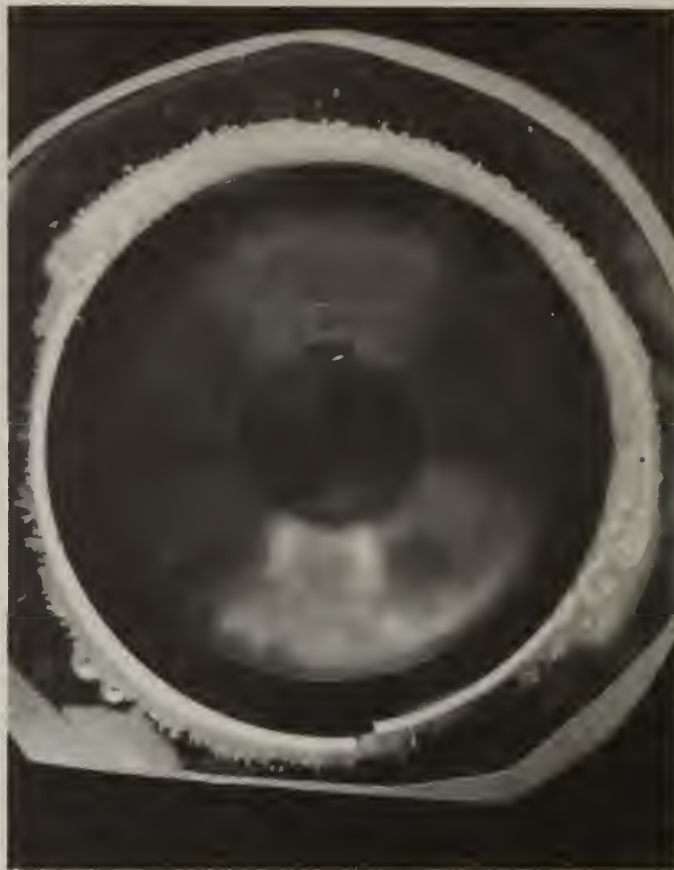


Fig. 2. Section of Type 316 stainless steel tubing after exposure to  $K_2SO_4$  seeded fuel rich hot gas stream. Note thin deposit on upper surface. Tube temperature 590 °C. 6 X.





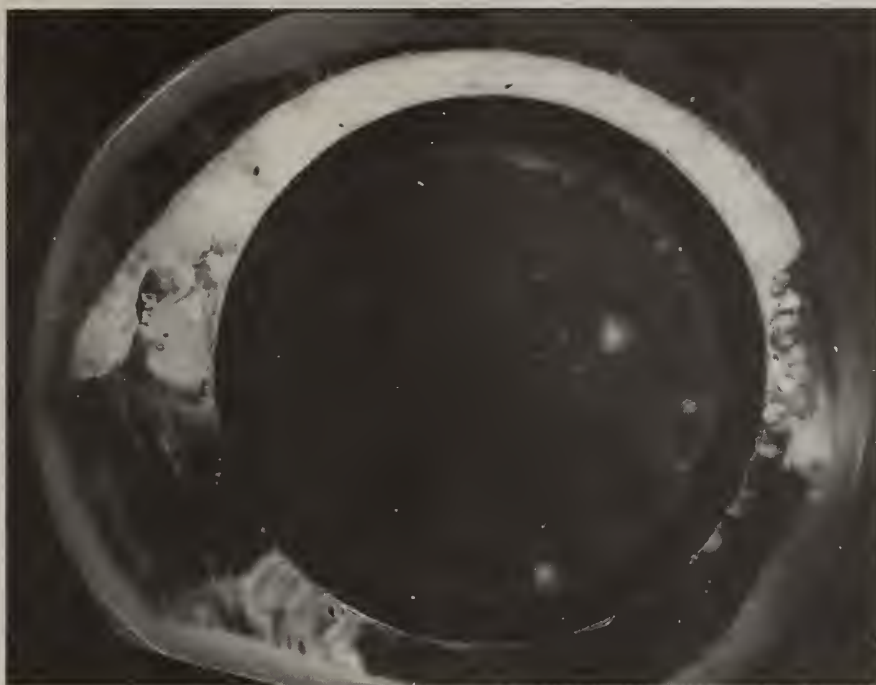


Fig. 3. Section of Type 316 stainless steel tubing after exposure to  $K_2SO_4 + K_2CO_3$  seeded  $O_2$  rich hot gas stream. Note thick deposit on upper surface. Tube temperature 500 °C. 6 X.

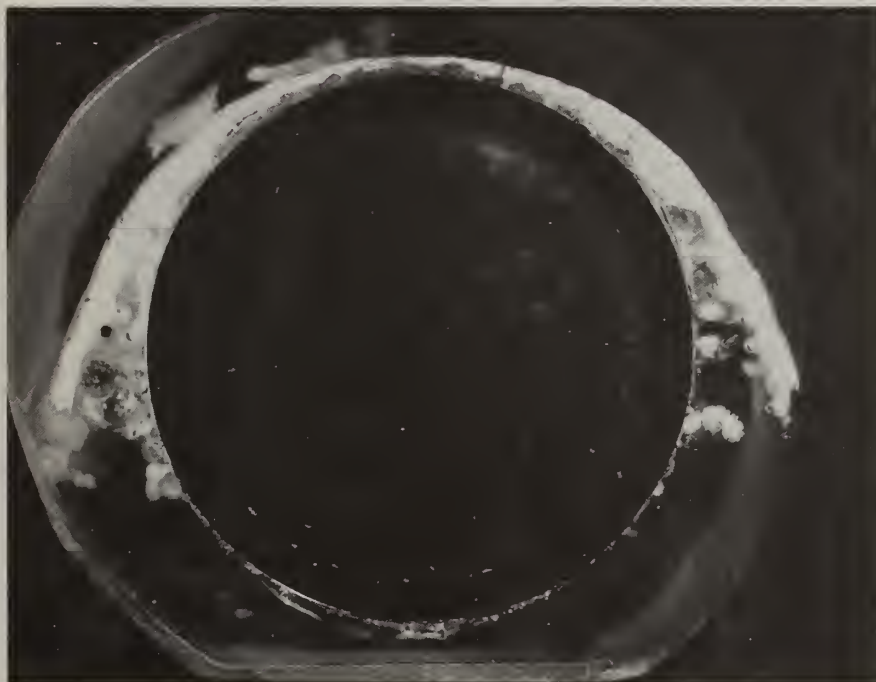


Fig. 4. Section of Type 316 stainless steel tubing after exposure to a  $K_2SO_4 + K_2CO_3$  seeded  $O_2$  rich hot gas stream. Tube temperature 590 °C. 6 X.





Fig. 5. Section of Type 316 stainless steel tubing after exposure to a  $K_2SO_4 + K_2CO_3$  seeded fuel rich hot gas stream. Note deposit on lower surface. Tube temperature 500 °C. 6 X.

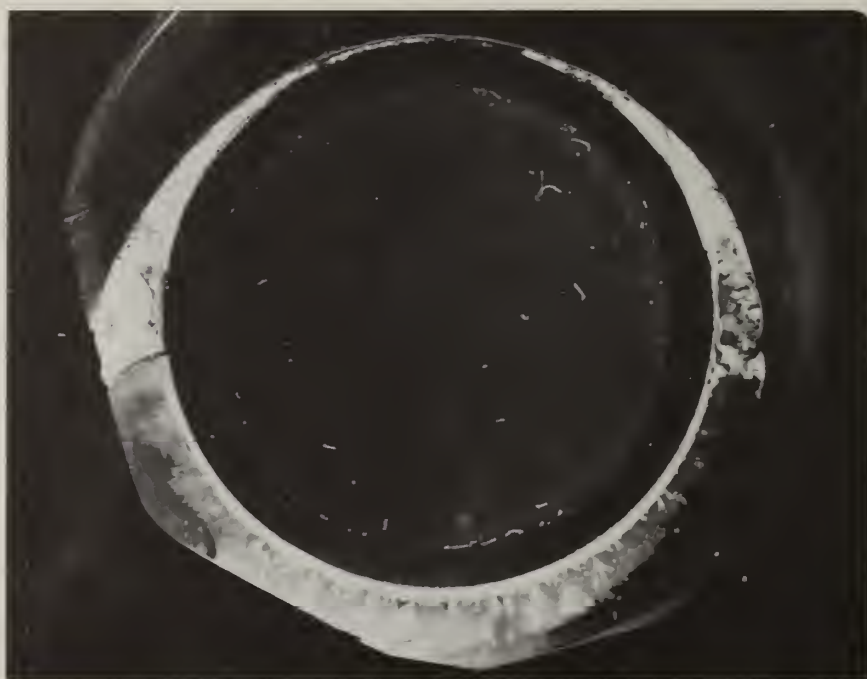


Fig. 6. Section of Type 316 stainless steel tubing after exposure to a  $K_2SO_4 + K_2CO_3$  seeded fuel rich hot gas stream. Tube temperature 590 °C. 6 X.



Fig. 7. Section of Type 304 stainless steel tubing after exposure to  $K_2SO_4$  seeded oxygen rich hot gas stream. Note formation of thick deposit, 2 mm, on upper surface and thin powdery deposit on lower surface. Tube temperature 400 °C. 6 X.



Fig. 8. Section of Type 304 stainless steel tubing after exposure to  $K_2SO_4$  seeded oxygen rich hot gas stream. Note formation of thick, 2 mm deposit on upper surface. Tube temperature 500 °C. 6 X.



Fig. 9. Section of Type 304 stainless steel tubing after exposure to  $K_2SO_4$  seeded oxygen rich hot gas stream. Note formation of thick deposit on upper surface. Tube temperature 590 °C. 6 X.

Fig. 10. Section of Type 304 stainless steel tubing after exposure to  $K_2SO_4$  seeded fuel rich hot gas stream. Tube temperature 400 °C. 6 X.



Fig. 11. Section of Type 304 stainless steel tubing after exposure to  $K_2SO_4$  seeded fuel rich hot gas stream. Tube temperature 500 °C. 6 X.

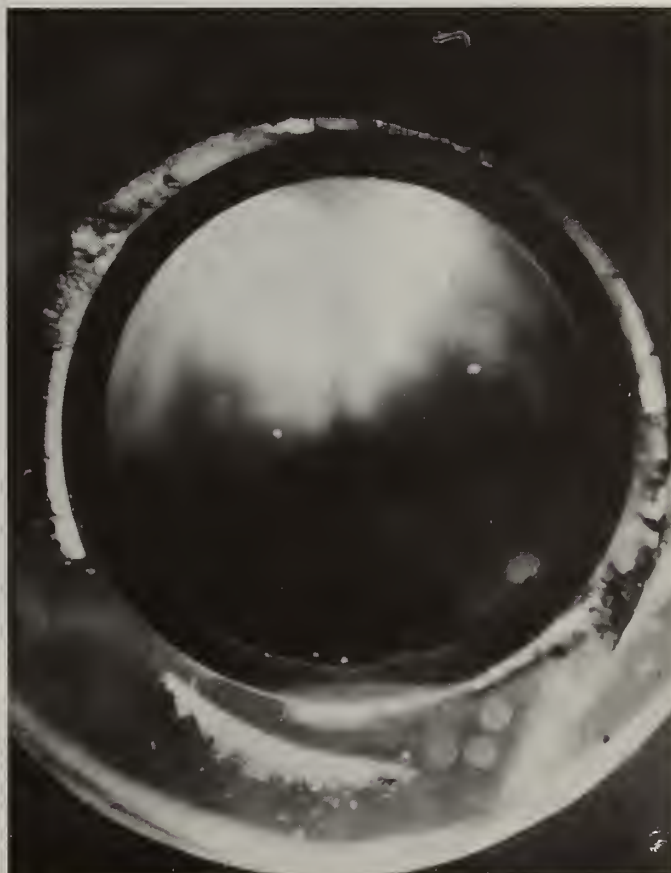






Fig. 12. Section of Type 304 stainless steel tubing after exposure to  $K_2SO_4$  seeded fuel rich hot gas stream. Tube temperature  $590^\circ C$ . 6 X.



Fig. 13. Section of Type 304 stainless steel tubing after exposure to  $K_2SO_4 + K_2CO_3$  seeded  $O_2$  rich hot gas stream. Note formation of thick, 1.7 mm, deposit on upper surface. Tube temperature  $400^\circ C$ . 6 X.





Fig. 14. Section of Type 304 stainless steel tubing after exposure to  $K_2SO_4 + K_2CO_3$  seeded oxygen rich hot gas stream. Note formation of thick, 1 mm, deposit on upper surface. Tube temperature 500 °C. 6 X.

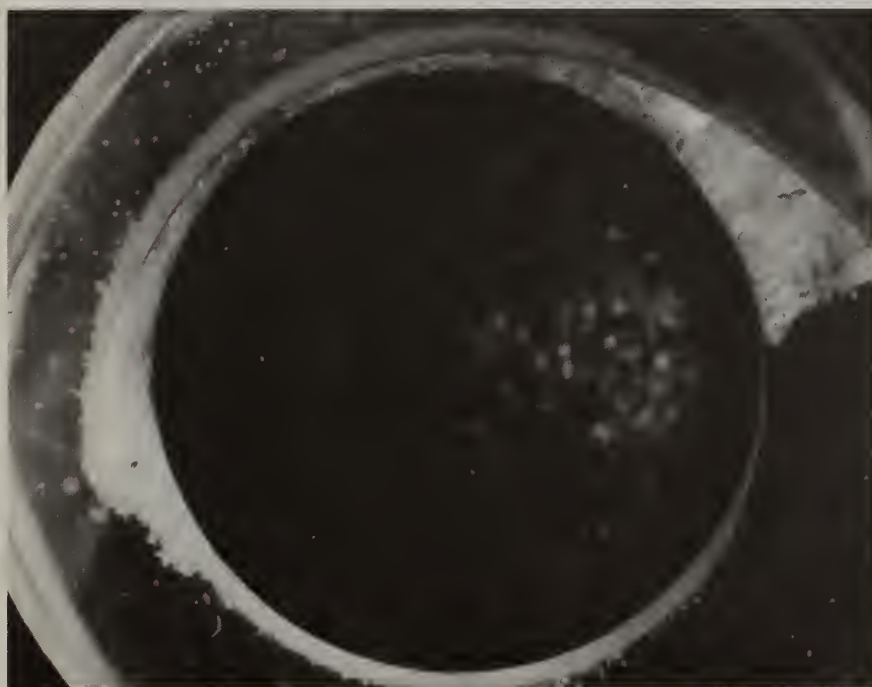


Fig. 15. Section of Type 304 stainless steel tubing after exposure to  $K_2SO_4 + K_2CO_3$  seeded oxygen rich hot gas stream. Note formation of thinner deposit on upper surface. Tube temperature 590 °C. 6 X.



Fig. 16. Section of Type 304 stainless steel after exposure to  $K_2SO_4$  +  $K_2CO_3$  seeded fuel rich hot gas stream. Note formation of 0.8 mm thick deposit on upper surface. Tube temperature 400 °C. 6 X.



Fig. 17. Section of Type 304 stainless steel tubing after exposure to  $K_2SO_4$  +  $K_2CO_3$  seeded fuel rich hot gas stream. Tube temperature 500 °C. 6 X.



Fig. 18. Section of Type 304 stainless steel tubing after exposure to  $K_2SO_4 + K_2CO_3$  seeded fuel rich hot gas stream. Note deposit on lower surface. Tube temperature 590 °C. 6 X.

